Nigerian Journal of Physics (NJP)
ISSN online: 3027-0936
ISSN print: 1595-0611
DOI: https://doi.org/10.62292/njp.v35i2.2026.471
Volume 35(2), June 2026

Indoor Radon Mapping and Assessment of Excess Lifetime Cancer Risk in the Kolmani Oil Field of Alkaleri, Bauchi State, Nigeria

***Alameen Mustapha Muhammed, Abdulkadir Adamu, Aliyu Mohammed Aliyu, Dauda Abubakar, Auwal Baballe and Abubakar Abba Aji**

Department of Physics, Sa'adu Zungur University, Bauchi State, Nigeria.

*Corresponding Author's Email: alaminmustapha37@gmail.com Phone No.: +2347016393453

ABSTRACT

Oil and gas exploration is one of the major sources of naturally occurring radioactive materials (NORMs). The work assessed the radiological hazard associated with the radon in soils of the oil and gas exploration site, Bauchi state, Nigeria. The study aims to measure indoor radon concentration and evaluate the excess lifetime cancer risk from its exposure. The indoor radon concentrations were measured at Kolmani oil field using electronic semiconductor detector (RAD7). The indoor radon activity concentration varies from 52.1 ± 1.92 Bq/m^3 to 196.5 ± 4.41 Bq/m^3 with a mean value of 126.5 ± 3.36 Bq/m^3. The result for Annual effective dose (E_{aed}) calculated from the measured indoor radon was 2.29 mSv/y, which are clearly above the permissible limit of 100 Bqm^{-3} and 1.15 mSv/y set by (WHO) and (UNSCEAR, 2000). The potential health risk was determined by computing Excess Lifetime Cancer Risk (ELCR) and lung cancer cases per year per million persons (LCC). The map for the distribution and exposure rate due to indoor Radon for the Kolmani oil field was also plotted using Golden surfer 12 software. The average values for (ELCR) and (LCC) are respectively1.2 x 10^{-2} and 56.28 per millions, which is lower than the limit range of 170–230 per million persons recommended by ICRP. These measurements provide valuable insights for evaluating public radiation exposure and establishing robust radiological safety protocols.

Keywords:
Indoor,
Radon,
Mapping,
Lifetime Cancer Risk,
Kolmani Oil Field.

INTRODUCTION

Naturally occurring radioactive materials (NORMs) are radionuclides that are present at varying concentrations in the earth's crust and can be concentrated and enhanced by processes such as the exploration of oil and gas (Xhixha et al., 2015). Crude oil and its products and wastes belong to the major sources of naturally occurring radioactive materials (NORMs), these products can then be enriched to some levels due to technological and human processes (Khandaker et al., 2018). Natural radioactivity is widely spread in the earth's environment and depends primarily on the geological and geographical conditions, and appears at different levels in the soils of each region in the world. Radionuclides derived from uranium and thorium, along with their decay products, are the most significant NORMs in radiological studies because they greatly contribute to human exposure in the environment (Isinkaye and Emelue, 2015).

. Several studies have confirmed that exposure to NORMs during the mining and production of oil and gas poses significant health and safety risks (Hanfi et al., 2021). More human evidence of the harmful nature of ionizing radiation was also reported by early radiologists and persons working in the Radium industry. Both empirical observations and epidemiological studies have consistently shown carcinogenic properties of ionizing radiation. Survivors of the Hiroshima atomic bomb exposed to radiation above one Sievert showed a significant increase in the incidence of leukemia (Yalcin et al., 2020).

Radon is an imperceptible, naturally occurring radioactive gas emitting alpha radiation. It arises from the decay of ^{226}Ra, a long-lived radionuclide with a 1600-year half-life, within the ^{238}U radioactive decay series. ^{222}Rn decays emit 5.49 MeV alpha particles, producing a series of radionuclides, primarily ^{214}Po and ^{218}Po, which contribute more than 90% of the total radiation dose associated with radon exposure (Adelikhah et al., 2021).

The primary source of indoor radon is uranium, which is found in drinking water, building materials, and the rocks and soil beneath homes. Long-term exposure to high indoor radon concentrations can have pathological consequences and functional respiratory alterations, raises the possibility of getting lung cancer (Qureshi et al., 2014).

Radon is the largest contributor to human radiation exposure, responsible for more than half of the global average annual dose. Regulatory actions and mitigation strategies are essential to address radon risks, necessitating comprehensive knowledge of radon levels and geographic distribution (Yousef and Zimami, 2019). Countries worldwide have implemented Radon mapping techniques to identify areas of elevated exposure risk. The maps serve as essential tools for radon risk assessment and mitigation in housing development (Loffredo et al., 2021).

Measuring indoor radon is vital, as it contributes significantly to the total natural radiation exposure, exceeding 50% of the overall dose (Coletti et al., 2022). Extensive research has been published recently on radon measurements worldwide and epidemiological investigations exploring the link between indoor radon exposure and lung cancer risk (Sheen et al., 2016). Workers and members of the public are liable to exposure from these radioactive materials if adequate radiation protection measures are not put in place. Nigeria is among the countries impacted by exposure to NORMs, particularly during exploration activities. Thus, the risk of exposure to radiation is often ignored. In the meantime, oil and gas exploration activity is being carried out in Bauchi State, it is therefore important to assess the presence of radionuclides in soils of the oil and gas exploration site so as to document the present radiological levels for environmental monitoring and protection as well as public health protection purposes. Existing literature indicates that no research has been conducted to assess the health risks from indoor radon exposure stemming from the granite quarry of the study area. The study intends to assess indoor radon concentrations and evaluate the excess lifetime cancer risk resulting from prolonged exposure. The research is aims to investigate the indoor radon concentration and also to measure gamma dose in the Kolmani oil field of Alkaleri to serve as a radiological assessment and improve health standard to the public.

MATERIALS AND METHODS

This section outlines the research methodology implemented to achieve the study's objectives. It includes a description of the study area, focusing on its geographical location. Sample collection, preparation, and analysis were carried out following established standard procedures. The present research mainly focuses on the measuring indoor ^{222}Rn concentration and its associate health hazard using RAD7, alpha particle detector (Durridge co, USA). The gamma dose rate was measured above 100cm from the ground level, using portable detector model 19, micro Roentgen (μR) meter. Finally, Multivariate statistical approaches (Pearson correlation) was employed to investigate the correlation between indoor radon concentration and measured gamma dose rate.

Study Area

The study area lies in the southeastern part of Bauchi area in Northeastern Nigeria, in the *Alkaleri Local Government area falls* within Latitude 10°7'03.9" N and Longitude 10°42' 43.8" E (fig 3.1). It is more specifically located at a border town between Bauchi and Gombe State called Kolmani village, a densely populated area. Two distinct seasons, dry and arid, characterize the study area. The rainy season starts from April and ends in October, while the dry season runs from November to March. The area is characterized by a few hills reaching an elevation of 706 m above sea level in the southwestern and northwestern regions, underlain by crystalline basement rocks. The lowest elevation in area is 275 m and it is associated with stream channels in the northeastern and southeastern regions, underlain by the Tertiary Kerri–Kerri Formation. The geology of the study area is somewhat complex as it coincides with the geological transition zone, between the Precambrian Basement Complex rocks in the northwestern and southwestern portions of the study and Tertiary sediments of the Upper Benue Basin which underlie the northeastern and the southeastern parts.

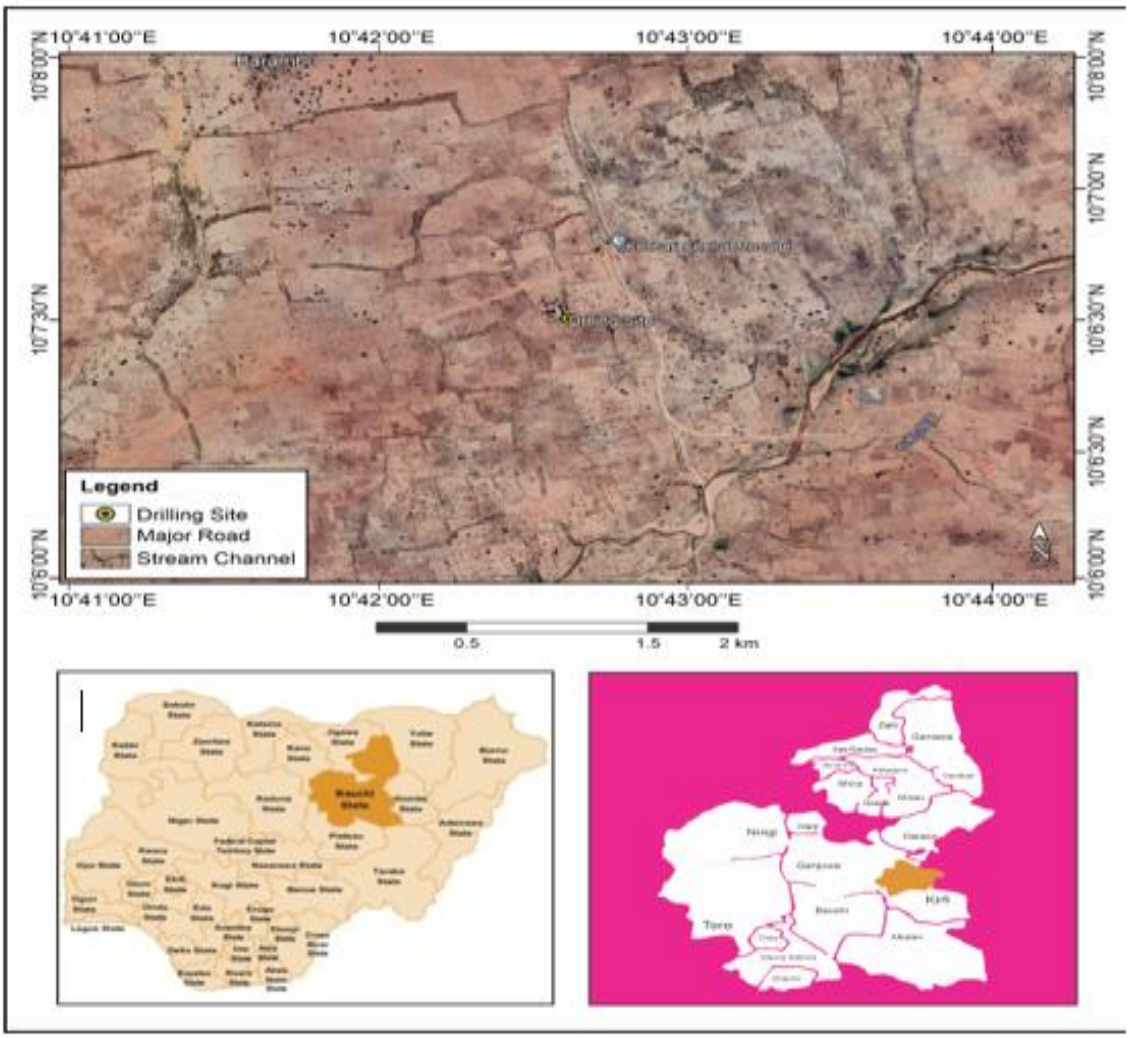

Figure 1: An Extracted Google Earth Map Showing the Geographical and Geological Description of the Study Area

Measurement of Radon in the Indoor and Soil Gas

The indoor radon concentrations were measured at 20 different locations across the study area with a special accessory for the purpose of measurement by the RAD-7 detector. The radon and thoron content in air is measured by the RAD-7 detector, a high-performance continuous radon measuring instrument simultaneously in thoron mode. Air is sucked by the built-in pump which is passed through the drierite to internal sample cell for the measurement of radon and thoron concentration. The detector distinguishes alpha particles from ^{218}Po and ^{214}Po with energies 6.0 MeV and 7.9 MeV, respectively in the respective windows. In thoron measurement the sample pump runs in a continuous fashion, at a steady consistent flow rate. Flow rate affects the amount of thoron in the internal cell, since a significant fraction of the thoron decays in the sample intake system as well as within the instrument (Rahman, M. 2009). The soil gas sample at each site is collected with the help of a probe, immersed in the soil to a depth of about 1 m, which is then connected to the RAD-7 detector with a special accessory for the purpose. The thin probe of app. 20 mm diameter is penetrated in the soil with a rotating handle or immersed with gentle strokes of a hammer. The water protected measuring instrument is then attached to the probe for sucking the soil gas from the deep soil. The soil gas is sucked through the tube pipe into the measuring instrument for 5 min pumping phase and then the data along with the respective bar charts and cumulative spectra of each sample are printed out on the printer attached with the instrument. During soil gas samplings, sniff protocol and Grabmode are used (Abuelhia, 2017).

Instrumentation

The RAD-7 Electronic Radon Detector (Durridge Co.) is a solid-state alpha detector. The schematic diagram of soil gas monitoring using RAD7. A solid-state detector is a semiconductor material (usually Silicon) that converts

alpha radiation directly to an electrical signal. The internal sample cell of RAD-7 is a 0.7 dm3 (0.7 l) hemisphere, coated on the inside with an electrical conductor. A solid state, ion implanted, planar Silicon alpha detector is at the centre of the hemisphere. The high voltage power circuit charges the inside conductor to a potential of 2000–2500 V relative to the detector, creating an electric field throughout the volume of the cell. The electric field pushes the positive charges onto the detector.

Working Principle of RAD7

The schematic drawing of the detector can be seen in Figure 2, there are three main components:

i. Air filter, that blocks the radon daughters out from the detector chamber,
ii. Air pump that makes the air circulate across the pipe system,
iii. Detector chamber, the main part of the detector, there is electrostatic field in the chamber that pushes the positive ions down onto the semiconductor detector, which is placed in this chamber.

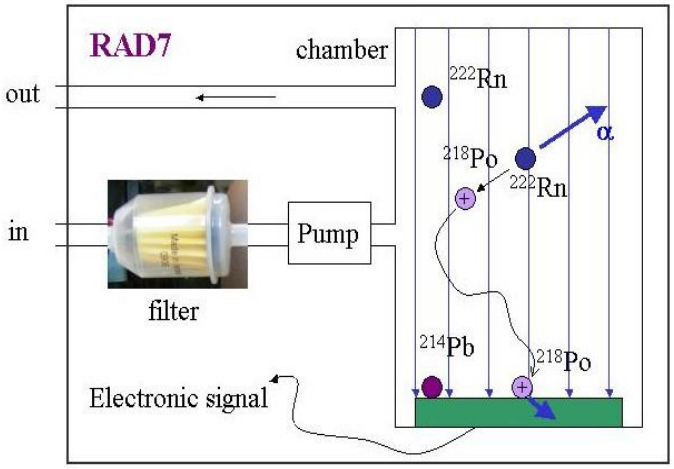

Figure 2: The Schematic Diagram of RAD7 and the principle operation of the Chamber

Radon decay in the chamber produces positively charged ^{218}Po ions, which are driven by an electric field onto a semiconductor detector. The detector measures the energy of alpha particles, while beta particles pass through without fully depositing energy. Signals are processed and stored by the RAD7 microprocessor, forming an energy spectrum that identifies polonium isotopes from radon and thoron decay chains. Since ^{218}Po has a short half-life (~3 minutes), its decay helps determine radon concentration using a differential equation (Yusuf et al., 2019).

$$\frac{dC(t)}{dt} = -\lambda C(t) \quad (1)$$

$$\frac{dC_{po}(t)}{dC} = \lambda_{po} C(t) - \lambda_{po} C_{po}(t) \quad (2)$$

C (t): represents activity concentration of radon in the detector chamber, and λ its corresponding decay constant. Also $C_{po}(t)$ and λ_{po} denote the concentration and decay constant of polonium-218 respectively.

When air is pumping into RAD7, there will be a time when the radon concentration in the surrounding C_O, will be equal to that of RAD7.

Therefore equation 2, becomes,

$$d\,C_{Po}(t)\,dt = \lambda_{Po} C_o - \lambda_{Po} C_{Po}(t) \quad (3)$$

By solving equation 3 and applying initial condition,

$$C_{Po}(t) = C_0 \quad (4)$$

Activity concentration of Radon can be obtained from equation 4, which illustrates the theoretical operation of RAD7.

Measurement of Terrestrial Gamma Radiation Dose (TGRD) Rates

A total of 20 gamma dose rate was measured across the study area. Three set of readings were taken at each measuring location in order to minimize measurement error with the average of each set recorded for each location alongside its coordinates. The (TGRD) at each location was measuerd and recorded at a height of 1 m above the ground, using portable detector, Radiation alert (mR) meter, manufactured by Radiagem, 2000 Geiger-Mueller counter. The device is designed for a wide range of applications including dose rate measurements in field conditions, in nuclear industry and for protection against radiological hazards by personnel in working environment. The longitute and latitute of each sample point were recorded using Global positioning system (GPS). The meter readings were in mili roentgen per hour, and the mean TGRD readings were converted to nGyh^{-1} using the recommended conversion factor of 1 µR h^{-1} to 8700 nGyh^{-1}

Data Analysis (Radiological Hazards Assessment)
Various radiological hazards parameters like the annual effective dose due to indoor ^{222}Rn concentration were calculated to assess the radiation risk to the public and analyze probable radiological hazards.

Statistical Analysis
The data obtained was analyzed using One-way analysis of variance (ANOVA). All the data will be computed as means ± standard deviation using statistical program SPSS 24.0 (Statistical Package for the Social Sciences).

Mapping the Distribution of Indoor ^{222}Rn
The Surfer 12 software was used for mapping the distribution of indoor radon concentration in the study area, to extract the maps of the study area and select sampling points based on geological formations. The contour and 3D surface maps depicted locations that are likely prone to an increase concentration of indoor ^{222}Rn.

RESULTS AND DISCUSSION
This section explains the results obtained in situ measurements of indoor radon concentration and terrestrial gamma radiation dose (TGDR) in 20 different locations across the study area, which widely cover all the geological formations. The gamma dose rate at each location was measured and recorded at a height 1 m from the ground, using Radiation alert inspector (mR/hr) survey meter, the readings obtained for gamma dose rate were used in computing the annual effective dose and lifetime cancer risk. The Surfer 10 software was employed for the geological mapping of the measured terrestrial gamma radiation dose (TGRD) in the study area.

Indoor Radon Concentration
The Indoor radon concentration of twenty different location of Kolmani oil field, Bauchi State Nigeria are presented in the Table 4.4. The data presents values for the indoor radon concentration, mean, and standard error. The activity concentration of the Indoor radon varies from 52.1 ± 1.92 Bq/m^3 to 196.5 ± 4.41 Bq/m^3 with a mean value of 126.5 ± 3.36 Bq/m^3. Significant variability is observed in the measured data across different locations. The mean radon concentration is higher than the WHO recommended limits of 100 Bq/m^3. The highest radon activity concentration is observed at the sampling location S9, that sample location is situated nearer to the kolmani oil field than all the other sampling locations. Radionuclide concentration decrease with distance due dilution with uncontaminated material and atmospheric deposition radioactive dust.

Table 1: Indoor Radon Concentration, Annual Effective Dose (AED), Excess Lifetime Cancer Risk (ELCR) And Lung Cancer Cases per Year per Million Persons (LCC)

Location code	Longitude	Latitude	Indoor radon concentration (Bq/m^3)	Annual effective dose AED (mSv/y)	Excess Lifetime Cancer Risk (ELCR)	Lung cancer cases per year per million persons (LCC)
S1	10°16’14’’N	10°19’48’’E	88.3 ± 2.91	1.92	8.7 x 10^{-3}	43.13
S2	10°16’20’’N	10°19’46’’E	157.6 ± 3.72	2.37	1.5 x 10^{-2}	58.48
S3	10°16’13’’N	10°19’50’’E	101.2 ± 3.13	2.01	1.2 x 10^{-2}	49.06
S4	10°16’11’’N	10°19’41’’E	142.9 ± 3.50	2.17	1.3 x 10^{-2}	60.59
S5	10°16’10’’N	10°19’33’’E	67.5 ± 2.01	1.57	7.5 x 10^{-3}	36.20
S6	10°16’19’’N	10°19’27’’E	176.8 ± 4.27	2.91	1.6 x 10^{-2}	75.32
S7	10°16’30’’N	10°19’39’’E	134.7 ± 3.64	2.13	1.4 x 10^{-2}	56.75
S8	10°16’35’’N	10°19’47’’E	109.3 ± 2.97	1.98	1.0 x 10^{-2}	50.08
S9	10°16’26’’N	10°20’00’’E	196.5 ± 4.41	3.12	2.0 x 10^{-2}	96.39
S10	10°16’34’’N	10°19’57’’E	110.8 ± 3.42	2.62	9.6 x 10^{-3}	51.83
S11	10°16’36’’N	10°20’12’’E	145.9 ± 3.86	2.20	1.5 x 10^{-2}	58.71
S12	10°16’31’’N	10°20’17’’E	117.6 ± 3.43	2.43	1.1 x 10^{-2}	53.60
S13	10°16’26’’N	10°20’20’’E	163.2 ± 3.70	3.09	1.8 x 10^{-2}	67.52
S14	10°16’20’’N	10°20’09’’E	138 ± 3.91	2.77	1.3 x 10^{-2}	53.10
S15	10°16’24’’N	10°20’06’’E	91.4 ± 2.85	2.48	9.1 x 10^{-3}	48.94
S16	10°16’18’’N	10°19’57’’E	129.5 ± 3.09	1.87	1.2 x 10^{-2}	55.97
S17	10°16’20’’N	10°19’55’’E	52.1 ± 1.92	1.45	6.3 x 10^{-3}	31.56
S18	10°16’07’’N	10°19’46’’E	173.3 ± 4.17	3.1	1.9 x 10^{-2}	72.37
S19	10°16’17’’N	10°19’36’’E	119.2 ± 3.26	1.87	1.0 x 10^{-2}	54.46
S20	10°16’59’’N	10°19’34’’E	114.2 ± 2.94	1.64	9.9 x 10^{-3}	51.58
Average			126.5 ± 3.36	2.29	1.2 x 10^{-2}	56.28

The higher value of indoor radon of this study which could be attributed to the oil and gas exploration. ^{222}Rn activity concentrations exhibit spatial variability due to differences in soil type, geology, topography and local meteorological conditions.

Table 2: Mean Indoor Radon Concentration (Bq/M^3) for this Study Compared to Other Countries of the World

S/No	Country	Indoor radon concentration (Bq/m^3)	References
2	Greek	135	(Clouvas et al., 2011)
3	Iran	150	(Adelikhah et al., 2021)
4	Korea	70.8	(Park et al., 2018)
5	Pakistan	128	(Khan et al., 2012)
6	Nigeria (Kolmani)	126.5	Present Study

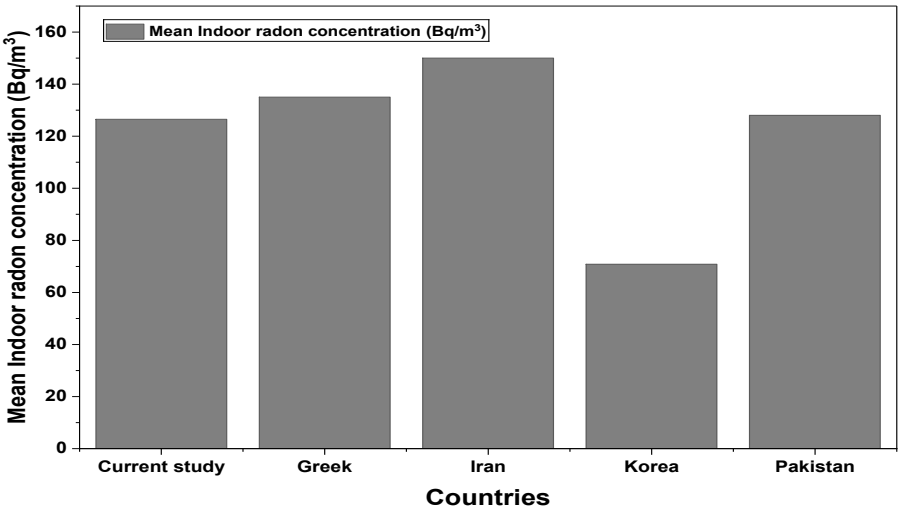

Figure 3: Comparison of The Mean Indoor Radon Concentration (Bq/M^3) Current Study with Previously Studied

The study conducted in the Saudi Arabia, the findings suggest that relative humidity positively influences radon concentration, as increased moisture in the air reduces radon diffusion and traps it indoors (Yousef and Zimami, 2019). In another study, the higher indoor radon can be attributed to Uranium and thorium content in the underlying earth, along with radon diffusion through soil and rock openings (Mehra and Bala, 2014). The concentrations of indoor radon and thoron are directly linked to the activity of ^{226}Ra and ^{232}Th in building materials, and indirectly influenced by soil composition and local geophysical characteristics which facilitates radon entry into dwellings (Adelikhah et al., 2021). Table 2 and Figure 3 show the Comparison between the mean activity indoor radon of the present study and previous studies, the mean activity indoor radon of the present study is higher than one reported in Korea (Park et al., 2018), yet is comparably lower reported in Greek (Clouvas et al., 2011) and Iran (Adelikhah et al., 2021), showing consistency with findings from research conducted in Pakistan (Khan et al., 2012).

Annual Effective Dose and Evaluation of Cancer Risk

The Radiological parameters such as annual effective dose (AED) , Excess Lifetime Cancer Risk (ELCR) and lung cancer cases per year per million person (LCC) through Indoor radon exposure were computated using equations 5, 6 and 7 respectively.

$$\text{AED (mSv/y)} = C_{\text{Rn}} \times \text{F} \times \text{T} \times \text{O} \times \text{DCF} \quad (5)$$

In the equation 5, C_{Rn} represents Indoor radon concentration (Bq/m^3), F is the equilibrium factor between radon and its daughters (0.4), O stands for occupancy factor (0.8), T is the Number of hours in a year (8760 h/yr) and DCF is the dose conversion actor (9×10^{-6} mSv/hr per Bq/m^3)(Ibrahim et al., 2023). The annual effective dose (AED) varies from 1.45 mSv/y to 3.12 mSv/y with a mean value of 2.29 mSv/y as tabulated on Table 4.1, Our findings indicate an average annual effective dose that is higher than the worldwide average of 1.15 mSv/y set by (Annex and Radiation, 2000). The results is in agreement with that reported by (Yousef and Zimami, 2019) and (Mehra and Bala, 2014).

The Excess Lifetime Cancer Risk is given by,

$$\text{ELCR} = \text{AED} \times \text{DL} \times \text{RF} \quad (6)$$

AED stands fo th the annual effective dose, DL is the average duration lifetime (70 years) and RF is the cancer risk factor (RF =0.05 Sv^{-1}). The Excess Lifetime Cancer Risk (ELCR) range from 6.3 x 10^{-3} to 2.0 x 10^{-2} with an average value of 1.2 x 10^{-2}.

Lung cancer cases per million people per year are calculated, based on a risk factor of 18×10^{-6} cases per million people per millisievert of radiation exposure.

$$LCC = DL \times 18 \times 10^{-6} \quad (7)$$

Lung cancer cases per year per million person (LCC) through Indoor radon exposure was computated to varies from 31.56 per million to 96.39 per million with a mean value 56.28 per million. The average (ELCR) and (LCC) were 1.4×10^{-2} and 70.07 per million, respectively, falling below the recommended limit of 170-230 cases per million persons set by the International Commission on Radiological Protection (ICRP) (Tirmarche et al., 2010).

Terrestrial Gamma Radiation Dose (TGRD)

The gamma dose rates were measured in a unit of mR h^{-1}, the readings were then converted to nGy h^{-1} using conversion factor (1 mR h^{-1} = 8.7 x 10^3 nGy h^{-1}). The mean values of gamma dose for 20 locations of the study are presented in table 4.3. The gamma dose rates ranged from 35.3 $nGyh^{-1}$ to 93.1 $nGyh^{-1}$ with a mean value of 66.76 $nGyh^{-1}$. The lowest gamma dose is found to be at sampling locations S17. The highest value was obtained at the sample point S9.

Table 3: Gamma Dose Rate in Different Locations across the Study Area

Location code	Gamma dose rate ($nGyh^{-1}$)	Annual effective dose AED (mSv/y)
S1	45.6	0.84
S2	80.4	2.08
S3	62.7	1.23
S4	71.5	1.72
S5	39.1	0.80
S6	85.3	2.25
S7	69.5	1.81
S8	49.2	1.16
S9	93.1	2.37
S10	63.7	1.40
S11	74.7	1.93
S12	67.3	1.65
S13	87.8	2.18
S14	70.2	1.69
S15	47.3	0.93
S16	66.6	1.57
S17	35.3	0.72
S18	89.6	2.26
S19	68.9	1.61
S20	67.3	1.59
Average	66.76	1.59

The mean of gamma radiation dose obtained from the study is higher than the average worldwide dose rate (59 $nGyh^{-1}$) (Sanusi et al., 2014). The mean value of gamma dose rate obtained from this studied was compared with the values obtained by other scholars from different nationalities as shown in the Table 4 and Figure 4, respectively. It can be clearly seen that the dose rate obtained in the present work is lower than that obtained in Malaysia (Ramli, 1997), Brazil (Anjos et al., 2011), Iran (Saghi et al., 2019) and Jordan (Alomari et al., 2019).

Table 4: Mean Dose Rate for This Study Compared to Other Countries of the World

S/No	Country	Gamma radiation dose rate ($nGyh^{-1}$)	References
2	Brazil	125	(Ramli, 1997)
3	Jordan	90	(Anjos et al., 2011)
4	Iran	118	(Saghi et al., 2019)
5	Malaysia	155	(Alomari et al., 2019).
6	Nigeria (Kolmani)	66.76	Present Study

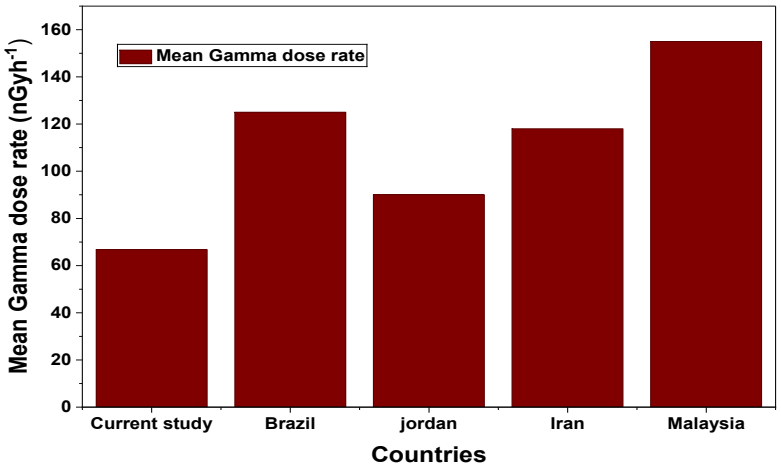

Figure 4: Comparison of the Mean Gamma Dose Current Study with Previously Studied

The total annual effective dose equivalent AE due to gamma dose is found to be $1.59 mSv\ y^{-1}$. The result is comparatively lower than the reported value of 1.64 mSv/y by (Jwanbot et al., 2013) and 1.50 mSv/y by (Karahan and Bayulken, 2000), and also the is lower than the worldwide average of 2.4 mSv/y (Sanusi et al., 2014).

Relationship between Indoor Radon Concentration and Gamma Dose Rate

A statistical parameter known as correlation was employed to investigate the relationship between measured indoor radon concentration and gamma dose rate as shown in the figure 4.3, the correlation coefficient is found to be R =0.93 which show there is strong relationship between measured radon concentration in soil and the gamma dose rate. The strong positive ccorrelation coefficients indicate that the gamma dose rate can be a good indicator of the geogenic radon potential (Tchorz-Trzeciakiewicz and Rysiukiewicz, 2021).

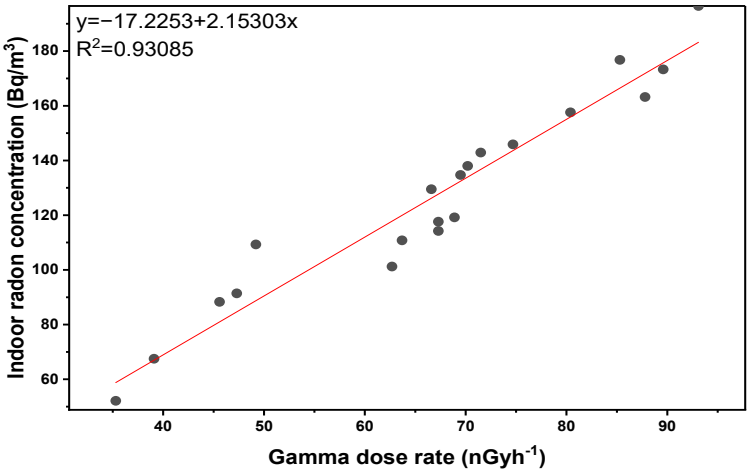

Figure 5: Relations between Measured Indoor Radon Concentration in Soil and Gamma Dose

Indoor Radon Mapping

The spatial distribution of indoor radon exposure rates is depicted in Figure 4.4, resulting from the integration of measurement data and geographic coordinates using Surfer 12 software for spatial analysis and mapping. Surfer 12 software facilitated the mapping of the study area and guided the selection of sampling points according to geological formation features. The contour maps depicted locations that are likely prone to an increase indoor radon exposure.

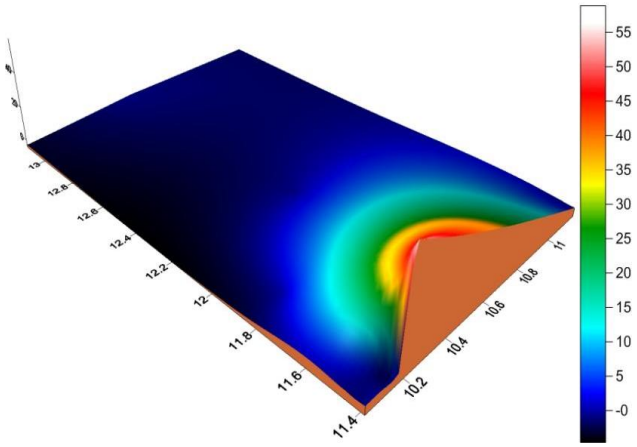

Figure 6: Contour Map for Indoor Radon of the Study Area

The Barnet model (Barnet et al., 2008) was applied to categorize Indoor radon concentrations into three distinct index categories: low, medium, and high. Figure 4.4 illustrates the spatial distribution of radon indices, categorizing regions into low (less than 30 kBq/m³), medium (30-100 kBq/m³), and high (exceeding 100 kBq/m³) radon levels (Ajiboye et al., 2018). Based on the radon contour map plotted for the study area, the highest radon activity concentration is observed at the sampling location S9, which is represents by dark red on the countour map. Granite intracrustal rocks forms the primary geological foundation of the region. The the sampling location S17 has the lowest radon activity concentration which is represents by blue colour on the

CONCLUSION

The research aims to quantify indoor radon exposure and estimate the resultant lifetime cancer risk, enabling a comprehensive risk assessment. Indoor radon activity concentrations ranged from 52.1 ± 1.92 Bq/m^3 to 196.5 ± 4.41 Bq/m^3 with a mean value of 126.5 ± 3.36 Bq/m^3. Radon concentrations exceed WHO guidelines, with an average value higher than the recommended 100 Bq/m³. The calculated Effective Lung Cancer Risk (ELCR) and Lung Cancer Cases (LCC) were 1.2 x 10^{-2} and 56.28 per million, respectively, well below the ICRP's recommended threshold of 170-230 cases per million. The radiological assessment reveals that oil and gas exploration in the study area does not poses a significant health risk to the community from the radiation exposure. A visual representation of indoor Radon distribution and exposure rates was generated for the study area using Golden Surfer 12.

A statistical parameter known as correlation was employed to investigate the relationship between measured indoor radon concentration and gamma dose rate , the correlation coefficient is found to be R =0.93 which show there is strong relationship between measured radon concentration in soil and the gamma dose rate. The strong positive ccorrelation coefficients indicate that the gamma dose rate can be a good indicator of the geogenic radon potential

However, prolonged exposure to even relatively low and moderate levels of radon increases the risk of developing lung cancer. The created radon map will facilitate proactive planning and decision-making for radon mitigation strategies. As enshrined in the WHO guidelines, the nigerian government should establish a national refrence level for radon concentration to as serve as public awareness about the health risk from its long-term exposure.

REFERENCES

Abuelhia, E. (2017). Evaluation of Annual Effective Dose from Indoor Radon Concentration in Eastern Province, Dammam, Saudi Arabia. *Radiation Physics and Chemistry,* 140**,** 137-140.

Adelikhah, M., Shahrokhi, A., Imani, M., Chalupnik, S. & Kovács, T. (2021). Radiological Assessment of Indoor Radon and Thoron Concentrations and Indoor Radon Map of Dwellings in Mashhad, Iran. *International Journal of Environmental Research and Public Health,* 18**,** 141.

Ajiboye, Y., Isinkaye, M. & Khanderkar, M. (2018). Spatial Distribution Mapping and Radiological Hazard Assessment of Groundwater and Soil Gas Radon in Ekiti State, Southwest Nigeria. *Environmental Earth Sciences,* 77**,** 545.

Ali, K. K., Shafik, S. S. & Husain, H. A. (2017). Radiological Assessment of Norm Resulting From Oil and Gas Production Processing In South Rumaila Oil Field, Southern Iraq. *Iraqi Journal of Science***,** 1037-1050.

Alomari, A. H., Saleh, M. A., Hashim, S. & Alsayaheen, A. (2019). Assessment Of Health Risk Associated With Natural Gamma Dose Rate Levels And Isodose Mapping Of Jordan. *Radiation Effects and Defects in Solids*.

Anjos, R. M. D., Ayub, J. J., Cid, A. S., Cardoso, R. & Lacerda, T. (2011). External Gamma-Ray Dose Rate And Radon Concentration In Indoor Environments Covered With Brazilian Granites. *Journal of Environmental Radioactivity,* 102**,** 1055-1061.

Annex, D. & Radiation, U. N. S. C. O. T. E. O. A. (2000). Sources and Effects of Ionizing Radiation. *Investigation of me,* 125.

Appleton, J. (2007). Radon: Sources, Health Risks, and Hazard Mapping. *Ambio***,** 85-89.

Babikir, E., Hasan, H. A., Abdelrazig, A., Alkhorayef, M., Manssor, E. & Sulieman, A. (2015). Radiation Dose Levels For Conventional Chest And Abdominal X-Ray Procedures In Elected Hospitals In Sudan. *Radiation Protection Dosimetry,* 165**,** 102-106.

Barnet, I., Pacherová, P., Neznal, M. & Neznal, M. (2008). Radon in Geological Environment—Czech Experience Czech Geological Survey Special Papers.

Clouvas, A., Xanthos, S. & Takoudis, G. (2011). Indoor Radon Levels in Greek Schools. *Journal of Environmental Radioactivity,* 102**,** 881-885.

Coletti, C., Ciotoli, G., Benà, E., Brattich, E., Cinelli, G., Galgaro, A., Massironi, M., Mazzoli, C., Mostacci, D. & Morozzi, P. (2022). The Assessment of Local Geological Factors for the Construction of a Geogenic Radon Potential Map Using Regression Kriging. A Case Study from the Euganean Hills Volcanic District (Italy). *Science of the Total Environment,* 808**,** 152064.

Hanfi, M., Emad, B. M., Sayyed, M., Khandaker, M. U. & Bradley, D. 2021. Natural Radioactivity in The Prospecting Tunnel In Egypt: Dose Rate And Risk Assessment. *Radiation Physics and Chemistry,* 187**,** 109555.

Haruna, R., Saleh, M., Hashim, S., Hamzah, K., Zainal, J. & Sanusi, M. (2020). Assessment of Geogenic Radon Potential In Johor Malaysia. *Journal of Radioanalytical and Nuclear Chemistry,* 326**,** 1065-1074.

Ibrahim, S., Koki, F. S., Maibulangu, M. H. & Baballe, A. (2023). Terrestrial Gamma Radiation Dose (Tgrd) Levels in Northern Zone Of Bauchi, Nigeria: Mapping and Statistical Relationship between Gamma Dose Rates and Geological Formations. *Gadau Journal of Pure and Allied Sciences,* 2**,** 9-15.

Isinkaye, M. & Emelue, H. (2015). Natural Radioactivity Measurements and Evaluation of Radiological Hazards in Sediment of Oguta Lake, South East Nigeria. *Journal of Radiation Research and Applied Sciences,* 8**,** 459-469.

Isinkaye, M. O., Fasanmi, P. O., Osman, H. & Khandaker, M. U. (2025). Naturally Occurring Radionuclides and Potentially Toxic Elements in Mine Waters from Artisanal Mining Sites within Ife-Ilesha Schist-Belt in Nigeria. *Physics and Chemistry of the Earth, Parts A/B/C,* 139**,** 103902.

Jwanbot, D., Izam, M., Nyam, G. & John, H. (2013). Radionuclides Analysis Of Some Soils And Food Crops In Barkin Ladi Lga, Plateau State-Nigeria. *Journal of Environment and Earth Science,* 3**,** 79-87.

Karahan, G. & Bayulken, A. (2000). Assessment of Gamma Dose Rates around Istanbul (Turkey). *Journal of Environmental Radioactivity,* 47**,** 213-221.

Kemski, J., Klingel, R., Siehl, A. & Valdivia-Manchego, M. (2009). From Radon Hazard to Risk Prediction-Based On Geological Maps, Soil Gas and Indoor Measurements in Germany. *Environmental Geology,* 56**,** 1269-1279.

Khan, F., Ali, N., Khan, E. U., Khattak, N. U., Raja, I. A., Baloch, M. A. & Rajput, M. U. (2012). Study Of Indoor Radon Concentrations And Associated Health Risks In The Five Districts Of Hazara Division, Pakistan. *Journal of Environmental Monitoring,* 14**,** 3015-3023.

Khandaker, M. U., Asaduzzaman, K., Sulaiman, A. F. B., Bradley, D. & Isinkaye, M. O. (2018). Elevated Concentrations Of Naturally Occurring Radionuclides In Heavy Mineral-Rich Beach Sands Of Langkawi Island, Malaysia. *Marine Pollution Bulletin,* 127**,** 654-663.

Loffredo, F., Savino, F., Amato, R., Irollo, A., Gargiulo, F., Sabatino, G., Serra, M. & Quarto, M. (2021). Indoor Radon Concentration and Risk Assessment in 27 Districts of a Public Healthcare Company in Naples, South Italy. *Life,* 11**,** 178.

Louro, A., Peralta, L., Soares, S., Pereira, A., Cunha, G., Belchior, A., Ferreira, L., Monteiro Gil, O., Louro, H. & Pinto, P. (2013). Human Exposure to Indoor Radon: A Survey in the Region of Guarda, Portugal. *Radiation Protection Dosimetry,* 154**,** 237-244.

Mehra, R. & Bala, P. (2014). Estimation of Annual Effective Dose Due To Radon Level in Indoor Air and

Soil Gas in Hamirpur District Of Himachal Pradesh. *Journal of Geochemical Exploration,* 142**,** 16-20.

Park, T. H., Kang, D. R., Park, S. H., Yoon, D. K. & Lee, C. M. (2018). Indoor Radon Concentration in Korea Residential Environments. *Environmental Science and Pollution Research,* 25**,** 12678-12685.

Petermann, E., Bossew, P. & Hoffmann, B. (2022). Radon Hazard Vs. Radon Risk-On The Effectiveness Of Radon Priority Areas. *Journal of Environmental Radioactivity,* 244**,** 106833.

Qureshi, A. A., Tariq, S., Din, K. U., Manzoor, S., Calligaris, C. & Waheed, A. (2014). Evaluation of Excessive Lifetime Cancer Risk Due To Natural Radioactivity in the Rivers Sediments of Northern Pakistan. *Journal of Radiation Research and Applied Sciences,* 7**,** 438-447.

Rahman, S. & Anwar, J. (2008). Measurement of Indoor Radon Concentration Levels in Islamabad, Pakistan. *Radiation Measurements,* 43**,** S401-S404.

Ramli, A. T. (1997). Environmental Terrestrial Gamma Radiation Dose and Its Relationship with Soil Type and Underlying Geological Formations in Pontian District, Malaysia. *Applied Radiation and Isotopes,* 48**,** 407-412.

Rezaei, H., Zarei, A., Kamarehie, B., Jafari, A., Fakhri, Y., Bidarpoor, F., Karami, M. A., Farhang, M., Ghaderpoori, M. & Sadeghi, H. (2019). Levels, Distributions and Health Risk Assessment of Lead, Cadmium and Arsenic Found in Drinking Groundwater of Dehgolan's Villages, Iran. *Toxicology and Environmental Health Sciences,* 11**,** 54-62.

Saghi, M. H., Mohammadi, A. A., Ghaderpoori, M., Ghaderpoury, A. & Alinejad, A. (2019). Estimate The Effective Dose Of Gamma Radiation In Iran Cities: Lifetime Cancer Risk By Monte Carlo Simulation Model. *Environmental Geochemistry and Health,* 41**,** 2549-2558.

Sanusi, M., Ramli, A., Gabdo, H., Garba, N., Heryanshah, A., Wagiran, H. & Said, M. (2014). Isodose Mapping of Terrestrial Gamma Radiation Dose Rate of Selangor State, Kuala Lumpur and Putrajaya, Malaysia. *Journal of Environmental Radioactivity,* 135**,** 67-74.

Sheen, S., Lee, K. S., Chung, W. Y., Nam, S. & Kang, D. R. (2016). An Updated Review Of Case–Control Studies Of Lung Cancer And Indoor Radon-Is Indoor Radon The Risk Factor For Lung Cancer? *Annals of Occupational and Environmental Medicine,* 28**,** 9.

Sherafat, S., Mansour, S., Mosaferi, M., Aminisani, N., Yousefi, Z. & Maleki, S. (2019). First Indoor Radon Mapping and Assessment Excess Lifetime Cancer Risk in Iran. Methodsx, 6, 2205-2216.

Tchorz-Trzeciakiewicz, D. & Rysiukiewicz, M. (2021). Ambient Gamma Dose Rate as an Indicator of Geogenic Radon Potential. *Science of the Total Environment,* 755**,** 142771.

Tirmarche, M., Harrison, J., Laurier, D., Paquet, F., Blanchardon, E. & Marsh, J. (2010). Icrp Publication 115. Lung Cancer Risk From Radon And Progeny And Statement On Radon. *Annals of the Icrp,* 40**,** 1-64.

Xhixha, G., Baldoncini, M., Callegari, I., Colonna, T., Hasani, F., Mantovani, F., Shala, F., Strati, V. & Kaçeli, M. X. (2015). A Century of Oil and Gas Exploration in Albania: Assessment of Naturally Occurring Radioactive Materials (Norms). *Chemosphere,* 139**,** 30-39.

Yalcin, F., Ilbeyli, N., Demirbilek, M., Yalcin, M. G., Gunes, A., Kaygusuz, A. & Ozmen, S. F. (2020). Estimation of Natural Radionuclides' Concentration of the Plutonic Rocks in the Sakarya Zone, Turkey Using Multivariate Statistical Methods. *Symmetry,* 12**,** 1048.

Yousef, A. & Zimami, K. (2019). Indoor Radon Levels, Influencing Factors and Annual Effective Doses in Dwellings of Al-Kharj City, Saudi Arabia. *Journal of Radiation Research and Applied Sciences,* 12**,** 460-467.